

It follows²⁵ from Stern's theory that the Pauli spin paramagnetism should vary in the same way as the electronic specific-heat coefficient on alloying. Hurd²⁵ has found such a variation, but the value of K that he obtains, with some assumptions, is higher by a factor of 2 than that given by the specific-heat results. Hurd²⁵ has also obtained a value of K for the Cu-Au system which is considerably higher than the value obtained from somewhat sparse specific-heat data,^{18,26} but the difference here may be due, in part, to the difficulty¹⁸ in preparing completely disordered samples. Haga¹⁰ has shown that the electron-phonon interaction has no effect on the spin paramagnetism, and hence Hurd's results lend some support to the Stern mechanism, but the difference in values of K means that this support is only qualitative.

The observed variation of Debye temperature with composition (Fig. 5) is in the direction predicted by Kleppa²⁷ from the observation that the Ag-Au system has a negative entropy of mixing. If the electron-phonon

²⁵ C. M. Hurd, Phys. Rev. **165**, 816 (1968).

²⁶ D. L. Martin and N. Waterhouse (to be published).

²⁷ O. J. Kleppa, J. Phys. Radium **23**, 763 (1962).

interaction does vary with composition,¹⁰ this would presumably be reflected in the Debye temperatures.

CONCLUSION

The present work has confirmed the general shape of the variation of the electronic specific-heat coefficient with composition as predicted by Stern from the results of Green and Valladares on silver-rich alloys. Stern's theory considers only the electron-impurity interaction, whereas a rival theory by Haga considers only the variation of electron-phonon interaction with composition.

The discovery of a nuclear specific-heat term in non-magnetic cubic alloys was an unexpected outcome of this work.

ACKNOWLEDGMENTS

It will be clear that this work has relied very heavily on the services of the Analytical Chemistry Section, N.R.C., thanks being especially due to D. S. Russell, P. Tymchuk, and A. Desaulniers. I am also indebted to J. W. Fisher for his care in making the alloys, to Mrs. L. Lacroix for computing assistance, and to R. L. Snowdon for assistance with the experiments.

Electromigration in Zinc Single Crystals*

J. L. ROUBORT†

Department of Physics and Astronomy, Rensselaer Polytechnic Institute, Troy, New York 12181

(Received 24 July 1968)

The electromigration of high-purity Zn single crystals resistively heated in an argon atmosphere has been measured by the marker-motion technique in the temperature range of 360 to 395°C with current densities of $\sim 5 \times 10^8$ A/cm². The cylindrical specimens were selected with c axes oriented within 25° perpendicular or parallel to the direction of current flow. Accurate measurements of both longitudinal and transverse strain rates were used to calculate the anode-directed atom-drift velocity v_a , and hence the effective charge on the moving ion, Z^* . The effective charge is found to be anisotropic: $Z_{11}^*/f = -2.55 \pm 0.15$ and $Z_{11}^*/f = -5.6 \pm 0.4$, where f is the correlation factor, which has been shown to be approximately 0.78. The anisotropy of the ion velocities is in the opposite sense and is greater than the anisotropy of the diffusivities. This results from the large anisotropy of the effective charge due to the band structure. It appears that this is the first demonstration of the crystalline anisotropy of the electromigration driving force.

I. INTRODUCTION

WHEN a large current flows through a metal, the ions are acted upon by the direct electrostatic field and by the "wind" force due to the transfer of momentum from the moving charge carriers to the ions. These forces act on the activated defect complexes to bias their jumps, thus producing an electromigration of atoms relative to the lattice. Several theories¹⁻³ have

been proposed to explain this effect. In the nearly-free-electron case, Huntington³ derived an expression for the force on a diffusing ion given by

$$F = |e|E \left[Z - z \left(\frac{\rho_d}{N_d} \right) \left(\frac{N}{\rho} \right) \frac{m^*}{|m^*|} \right] = |e|EZ^*, \quad (1)$$

where e is the electronic charge, E the electric field, Z is the effective electrostatic charge on the moving ion, z the number of conduction electrons/atom, ρ_d is

* This work was supported by a grant from the U. S. Atomic Energy Commission.

† Present address: Metallurgy Division, Argonne National Laboratory, Argonne, Ill. 60439.

¹ V. B. Fiks, Fiz. Tverd. Tela **1**, 16 (1959) [English transl.: Soviet Phys.—Solid State **1**, 14 (1959)].

² C. Bosvieux and J. Friedel, J. Phys. Chem. Solids **23**, 123 (1962).

³ H. B. Huntington and A. R. Grone, J. Phys. Chem. Solids **20**, 76 (1961).

essentially the resistivity of all the defects, ρ the total resistivity, N_d the number of defects, and m^* the effective mass of the charge carriers. The force, though not directly measurable, may be estimated by measuring the drift velocity v_a of the ions which is related to the force by the Nernst-Einstein relation

$$v_a = DF/kT, \quad (2)$$

where D is the diffusion coefficient, k is Boltzmann's constant, and T is the absolute temperature.

In Fiks's¹ formulation, the effective charge Z^* may be written as

$$Z^* = (Z - n_e \sigma_e \Lambda_e + n_h \sigma_h \Lambda_h), \quad (3)$$

where n is the number of holes (n_h) or electrons (n_e), σ is the respective scattering cross section of the activated complex at the saddle-point position, and Λ is the respective mean free path. In the simple interpretation of experimental results, one would expect that if the "wind" effect were to dominate the electrostatic force, the direction of mass flow would depend on the sign of the predominant charge carriers. That is, ions in metals with negative Hall coefficients (electron conductors) would move towards the anode, while the situation would be reversed for hole conductors. For metals with large Hall constants, this is indeed the case, but the situation is not clear for metals with small positive Hall constants. Mass is observed to move towards the anode for Zn,^{4,5} Cd,⁵ and Pb.^{4,5} These metals all have a small positive Hall constants at room temperature. Only in the cases of Fe⁶ and Co⁷ is the mass flow directed towards the cathode in agreement with their large positive Hall constants.

All of the above mentioned experiments have been performed on polycrystalline material, but single crystals of Zn are quite anisotropic, not only in their diffusivities and low-temperature conductivity, but also in their Hall constants. The average values of the Hall constants of monocrystalline Zn at 78°K and room temperature as measured by Lane *et al.*⁸ are reproduced in Fig. 1. There is no clear, simple correlation between our results and these Hall constants. R_1 is the constant measured with the magnetic field parallel to the c axis. Therefore it depends on motion of the carriers in the basal plane as does our Z_1^* , while R_2 , which is the constant with the field perpendicular to the c axis, is related to some function of Z_1^* and Z_{11}^* . A simple model would predict that, since $R_1 > R_2$, then $Z_1^* > Z_{11}^*$, which is not the case.

Nevertheless, if one can extrapolate the measurements of Lane *et al.* to higher temperatures, there is a

⁴ P. Thernqvist and A. Lodding, *Z. Naturforsch* **21a**, 1311 (1966).

⁵ P. P. Kuzmenko, *Ukr. Fiz. Zhur.* **7**, 117 (1962).

⁶ H. Wever, *Electrolytic Transport and Conduction Mechanism in Iron and Nickel* (H. M. Stationery Office, London, 1959).

⁷ P. S. Ho, *J. Phys. Chem. Solids* **27**, 1331 (1966).

⁸ G. S. Lane, A. S. Huglin, and J. Stringer, *Phys. Rev.* **135**, 1060 (1964).

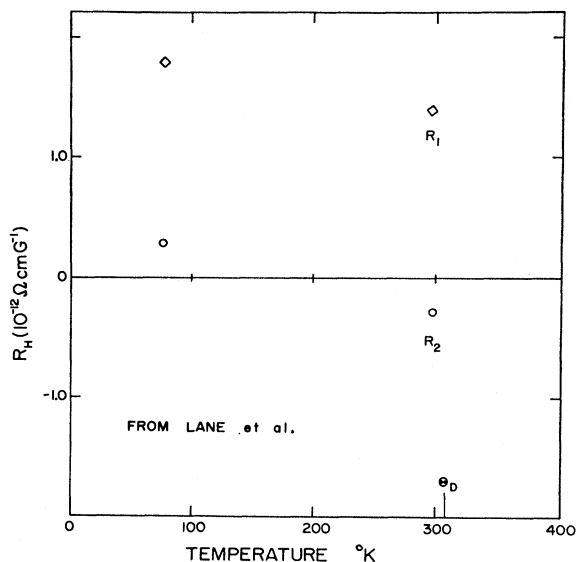


Fig. 1. Variation of Hall constants, R_H , versus T , from Lane *et al.* R_1 (data points indicated by \diamond) is the Hall constant when the field is parallel to the c axis, R_2 (data points indicated by \circ) is the Hall constant when the field is perpendicular to the c axis.

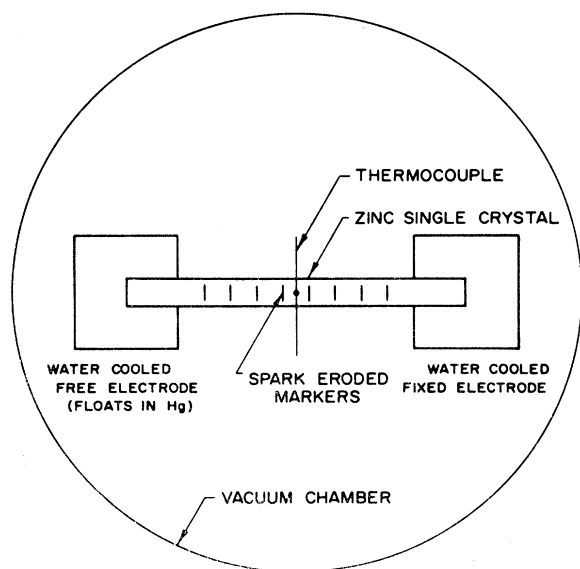
trend for both constants to become negative and hence we might expect anode-directed mass motion in an electromigration experiment in Zn. This investigation was stimulated in part by the electromigration with polycrystalline Zn,^{4,5} where the direction of mass flow ran counter to that expected from the Hall effect measurements also on polycrystals, and in part by the interesting implications in the Hall effect anisotropy as found in single crystals by Lane *et al.*

II. EXPERIMENTAL PROCEDURE

The two standard techniques for measuring electromigration in metals are the isothermal isotope technique as used by Gilder and Lazarus⁹ and the vacancy flux technique used by Huntington and Grone.³ The latter technique, while being less accurate and subject to more corrections, has the advantage of being applicable to a wider group of metals as well as being easier to use and more adaptable to survey purposes. The measurement of surface marker velocities has been used in this study to infer the atom drift velocities needed to calculate the effective charges of the moving ions.

A schematic view of the apparatus is shown in Fig. 2. Prior to mounting, small (40μ wide $\times \sim 100 \mu$ deep) scratches are produced on the surface of the specimen by a spark-erosion machine. A finely honed razor blade is used as the tool. This technique for producing the markers yields no recrystallization within the sample during the experiment. A crystal run for ~ 2 weeks at 380°C was polished and back reflection x rays taken at

⁹ H. M. Gilder and D. Lazarus, *Phys. Rev.* **145**, 507 (1966).



ELECTROMIGRATION APPARATUS

FIG. 2. Schematic view of electromigration apparatus.

several spots. No astigmatism or variation of orientation was detected. A 0.003-in.-diam chromel versus alumel thermocouple is spot-welded on the underside of the center of the crystal in the manner indicated to minimize the dc "pickup" generated by the current flow.

The specimen is then mounted between the two water-cooled copper electrodes, one of which is fixed and the other free to float on a mercury reservoir to allow for stress-free thermal expansion and alignment. The chamber and the power supply used has been described by Sullivan.¹⁰ Current densities of 5×10^3 A/cm² were typical. For these experiments, the chamber was evacuated to 5×10^{-3} Torr and then filled either with tank argon (99.996%) or purified tank argon (run through a CaSO₄ drying agent and a furnace filled with copper filings at 650°C), to a pressure of 1½ atm to reduce evaporation. The marker positions were measured to $\pm 1 \mu$ through a window once or twice a day by means of a traveling microscope, and the radial dimensions, which were measured at least twice during an experiment, were determined to $\pm 3 \mu$ by a filar eyepiece which moves perpendicular to the crystal axis. Good statistics were obtained by running the experiments from 7 to 14 days.

Only the temperature of the marker directly over the thermocouple is known to any accuracy. For these experiments only the datum obtained at the point where the thermocouple is attached is quoted. Melting-point calibrations agreed with the thermocouple output to within $\pm 2^\circ\text{C}$ if performed before diffusion of the thermocouple material into the Zn (which lowers its melting point) occurred.

¹⁰ G. A. Sullivan, Phys. Rev. 154, 605 (1967).

All Zn used was 99.999% pure obtained in the form of 1/8-in.-diam wires from Cominco Products, Inc. Wires 6 in. long were sealed at a pressure of 10^{-3} Torr in a precision bore tubing (0.125-in. i.d.) coated internally with a solution of Aguadag (product of Acheson Colloids Co.). These tubes were then run through a Bridgman-type furnace. The orientations were determined by Laue back reflection x rays to within $\pm 2^\circ$. The maximum distortion of the spot size was less than $\pm 1^\circ$. Only those crystals whose *c* axes were between 70° and 90° or between 0° and 24° to the axis of current flow were used. In the usual notation those crystals whose *c* axes were in the former category have been designated as \perp crystals. When the desired orientation was found, the crystal was cut into 2-in. lengths by an acid string saw, etched in 50% HCl, and mounted in a "V" block by a mixture of Duco cement and graphite for spark erosion. This mixture dissolves in acetone. Finally, the thermocouple was attached and the crystal mounted with 2.4 cm between the clamps. This free length gave the desired temperature using the available current of the power supply.

Several metallographic examinations were made to look for voids. The procedure adopted for this was to pot the specimen after the run in a mold of Epoxy resin. By carefully using various grades of emery paper and alumina powder with a polishing cloth, a scratch-free surface could be obtained. Finally the specimen was

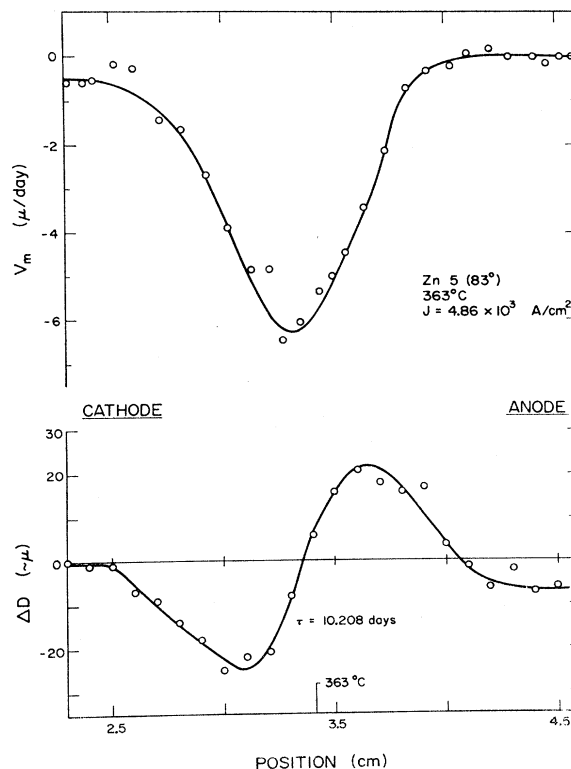


FIG. 3. Marker velocity and ΔD versus position for 83° crystal, $T = 363^\circ\text{C}$, $j = 4.86 \times 10^3$ A/cm².

electropolished in a mixture of equal parts of orthophosphoric and ethyl alcohol using stainless steel as the cathode. The specimen was examined in a conventional microscope.

III. EXPERIMENTAL RESULTS

A. Results

Figures 3-6 are the data from four typical experiments. The upper curves display the marker velocity as a function of position along the crystal. The point at which the thermocouple is mounted is indicated on the abscissa. The lower curve represents the radial dimensional changes, $D_f - D_i = \Delta D$, where D_i is the initial diameter and D_f the final diameter measured after a time τ . The temperature quoted is the average temperature and is accurate to $\pm 1^\circ\text{C}$, although somewhat larger ($\pm 4^\circ\text{C}$) deviations from the mean were occasionally observed because of a variation in the power supply output caused by room-temperature fluctuations.

The negative velocity indicates that the markers are moving towards the cathode. Since the markers are fixed to atomic planes, and move in the direction of the vacancy flux, the mass flow is towards the anode. The marker velocity is obtained by a least-squares fit to a displacement-versus-time curve for each marker. The

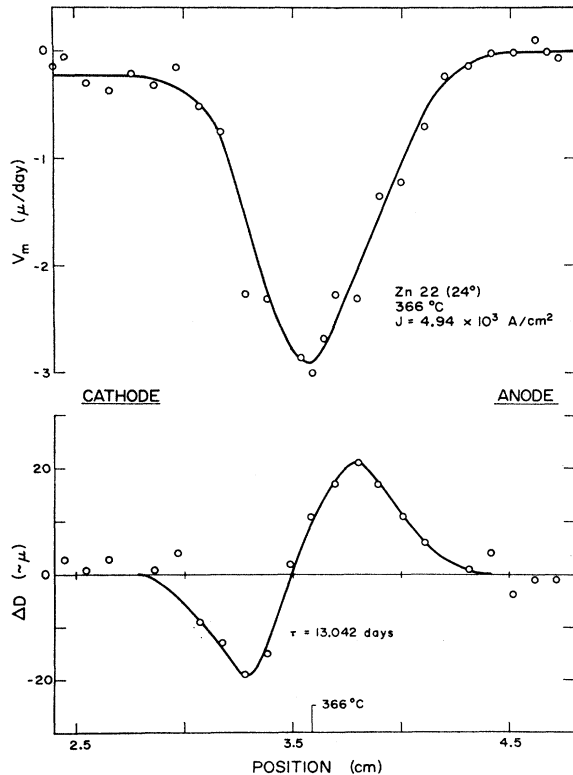


Fig. 4. Marker velocity and ΔD versus position for 24° crystal, $T = 366^\circ\text{C}$, $j = 4.94 \times 10^3 \text{ A/cm}^2$.

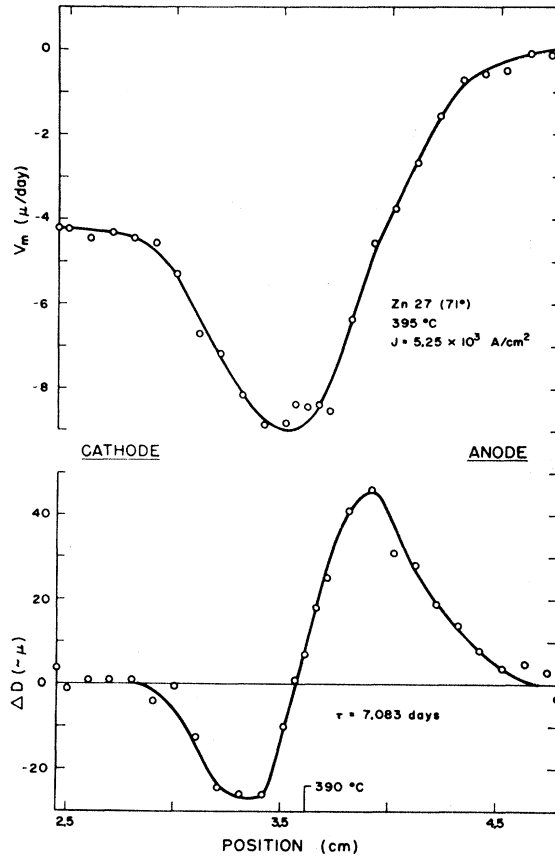


Fig. 5. Marker velocity and ΔD versus position for 71° crystal, $T = 395^\circ\text{C}$, $j = 5.25 \times 10^3 \text{ A/cm}^2$.

standard deviation of these points is typically less than $\pm 0.1 \mu/\text{day}$. The diameter changes are more difficult to measure and consequently the error in ΔD is $\pm 10\%$.

Figure 3 presents the results obtained on a crystal whose c axis was oriented 83° from the axis of current flow, run at a maximum temperature of 363°C with a current density of $4.86 \times 10^3 \text{ A/cm}^2$. The results obtained from a 24° crystal using a current density of $4.94 \times 10^3 \text{ A/cm}^2$, resulting in a maximum temperature of 366°C , are shown in Fig. 4. Similar experimental measurements at higher temperatures are shown in Figs. 5 and 6, under the conditions shown on the figures.

There are several common features of these results. At the same temperature the marker velocities are higher for \perp crystals than \parallel ones. The maximum velocity does not always occur at the geometrical center (the place where the thermocouple is attached), but is frequently shifted towards the cathode. (In a private communication, Lodding reports that he has observed this shift in polycrystalline Zn and Li.) The area under the curve on the anode side of the radial dimensional changes is greater than the area under the cathode side of the curve. All crystals show a net expansion, which is somewhat greater at higher temperatures.

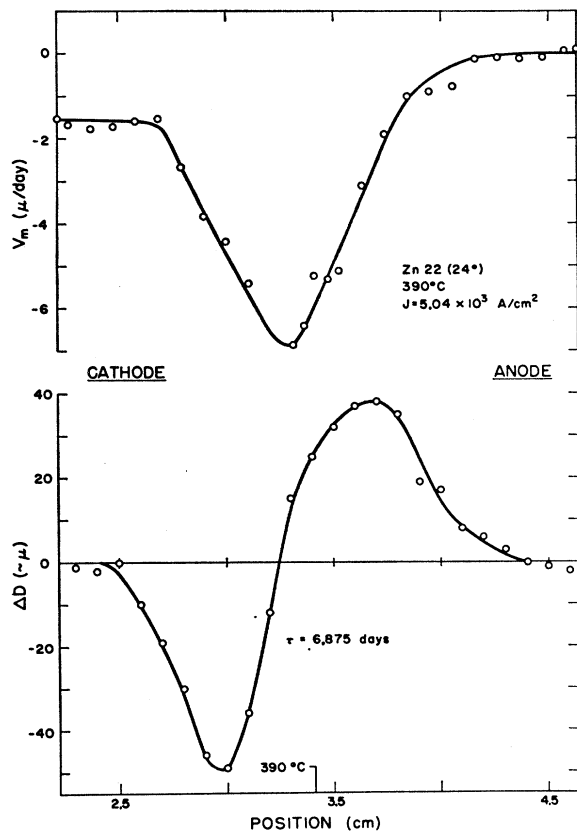


FIG. 6. Marker velocity and ΔD versus position for 24° crystal, $T = 390^\circ\text{C}$, $j = 5.04 \times 10^3 \text{ A/cm}^2$.

A temperature gradient will also cause mass motion. This Soret effect in Zn is small. Three measurements of the thermal mass transport¹¹⁻¹³ in polycrystalline Zn disagree among themselves even as to the direction of vacancy flux. Although our setup was not designed to measure thermomigration, two ac experiments were performed for this study with very inconclusive results because the mass motion was only slightly above the experimental resolution. These crystals did exhibit a net expansion which is not understood. Because of the small Soret effect, no correction for the thermal mass transport will be applied to the previously mentioned dc results.

B. Analysis

The common difficulty of all vacancy-flux-type experiments is that the atom drift velocity is not directly measurable as in the case of the isothermal-isotope-type experiments. From the conservation of mass, one can show that the atom drift velocity in isotropic materials is related to the marker velocity

¹¹ P. Shewmon, J. Chem. Phys. **29**, 1032 (1958).

¹² R. A. Swalin, W. C. Olander, and P. Lin, Acta Met. **13**, 1063 (1965).

¹³ T. F. Archbold and P. G. McCormick, Trans. Met. Soc. AIME **236**, 713 (1966).

v_m by¹⁴

$$v_a = - \int_0^x \dot{\Delta}(x) dx, \quad (4)$$

where $\dot{\Delta}(x) = \dot{\epsilon}_{xx} + 2\dot{\epsilon}_{rr}$ is the dilatation rate. The experimentally measured quantities are the longitudinal strain rate, $\dot{\epsilon}_{xx} = \Delta v_m / \Delta x$, and the radial strain rate, $\dot{\epsilon}_{rr} = \Delta D / D \tau$. In such an analysis it is assumed that evaporation, oxidation, and void formation can be neglected. In these experiments there is no evidence for evaporation, but an oxide film is observed to form on the crystal. It is also felt that voids are formed, which will be discussed below.

By defining an isotropy factor α as

$$\alpha = \epsilon_{xx} / (\epsilon_{xx} + 2\epsilon_{rr}), \quad (5)$$

and assuming α is not a function of position, the atom drift velocity becomes

$$v_a = - (1/\alpha) v_m. \quad (6)$$

As pointed out by Penny,¹⁴ α should lie between $\frac{1}{3}$ and 1; the former limit holds for completely isotropic dimensional changes. The isotropy factor can apparently be less than $\frac{1}{3}$ if either the surface acts as a vacancy source or sink or if there is plastic deformation caused by mechanical strains imposed on the specimen (as in the case of the constraints caused by the volume change which occurs during the β - γ phase transformation in uranium).¹⁵

Although the metallographic examination mentioned previously has revealed no voids, there is a strong indication from the over-all expansion and unequal areas

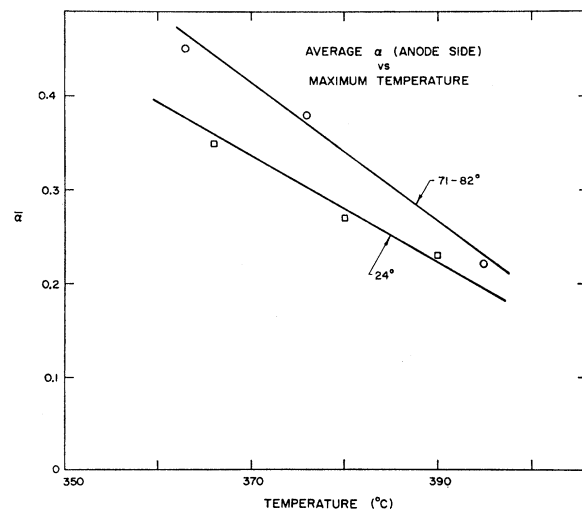


FIG. 7. Isotropy factors for \perp and \parallel orientations versus maximum temperature ($^\circ\text{C}$).

¹⁴ R. V. Penny, J. Phys. Chem. Solids **25**, 335 (1964).

¹⁵ J. F. D'Amico, Ph.D. thesis, Rensselaer Polytechnic Institute, 1964 (unpublished).

under the radial dimensional changes that they exist, possibly too small to examine optically. Because of the void formation, the exact formula (4) is not applicable in these experiments. Optical observations have occasionally revealed large voids¹⁶ on the cathode side of Ag during electromigration, owing to the clustering of vacancies at nucleation sites. In order to avoid the complications of voids, the isotropy factor has been calculated only on the anode side of the crystal, avoiding the central region, where it was felt that the oxide coat might influence the results. Over the anode side, α is found to be constant within $\pm 10\%$. Accordingly v_a can be calculated from Eq. (6) using a constant α for each experiment. The isotropy factors obtained in this manner are shown in Fig. 7. The interesting features which will be discussed in detail later are the dependence on orientation, the dependence on the maximum temperature, and the fact that several α 's measured at higher temperatures are less than $\frac{1}{3}$. This latter fact was also found to be true of a polycrystalline specimen run at a maximum temperature of 380°C.

Using Ohm's law (the resistivity ρ is isotropic at these temperatures) and Eqs. (2) and (6), one may write

$$DZ^* = -v_m kT / \alpha j \rho |e|, \quad (7)$$

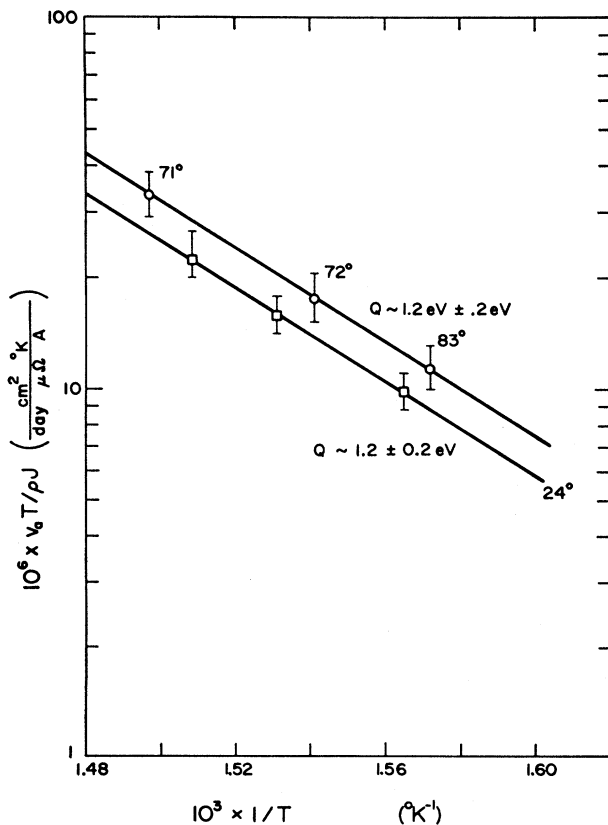


FIG. 8. $\ln(v_m T / \alpha j \rho)$ versus $1/T$.

¹⁶ P. S. Ho, Ph.D. thesis, Rensselaer Polytechnic Institute, 1968 (unpublished).

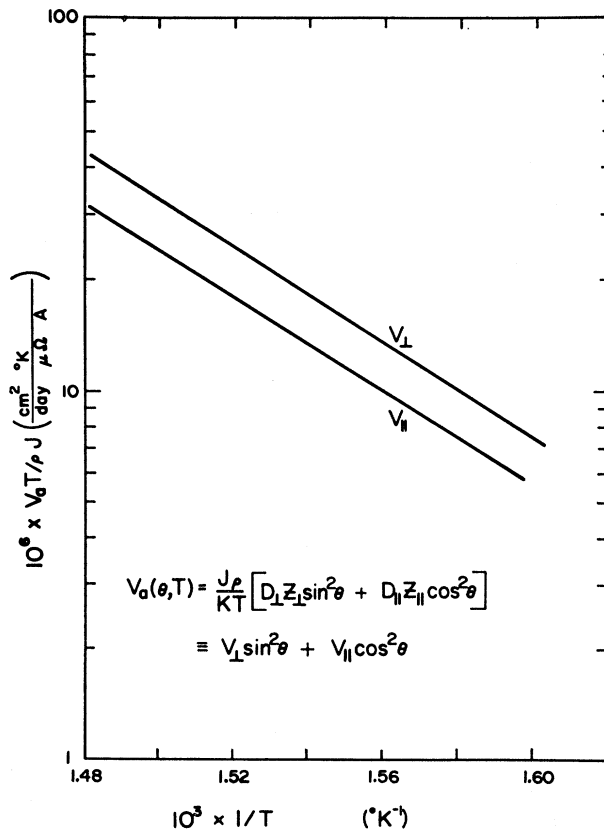


FIG. 9. $\ln(v_m T / \alpha j \rho)$ resolved by using $V_a(\theta, T) = (j \rho / k T) [D_{\perp} Z_{\perp} \sin^2 \theta + D_{\parallel} Z_{\parallel} \cos^2 \theta]$ onto \perp and \parallel directions versus $1/T$.

where j is the current density. The results of plotting $\ln(v_m T / \alpha j \rho)$ versus $1/T$ are shown in Fig. 8, where only the uncertainties in the isotropy factor are indicated by the error bars. The resistivity is taken from a National Bureau of Standards report.¹⁷ This Arrhenius plot yields activation energies of 1.2 ± 0.2 eV,¹⁸ in fair agreement with the self-diffusion measurements of Peterson and Rothman.¹⁹ This indicates that the marker motion is indeed a measure of bulk diffusion, which is implicit in the assumption that the markers are fixed to the atom planes. Figure 9 shows the resolution of the velocities of Fig. 8 onto the principal crystallographic axes. The equation used on the figure is self-explanatory.

In order to calculate Z^* from v_m , we must use the correlated diffusion constants that are measured from self-diffusion studies, where it is expected that the mechanism of diffusion is the same as in electromigration. When one uses these correlated diffusion constants,

¹⁷ Natl. Bur. Std. (U. S.), Circ. 395 (1931).

¹⁸ Recently the acquisition of an infrared detector has allowed a determination of the temperature at each marker on the crystal. Thus, it is possible to make an Arrhenius plot for each crystal. Using this technique, an activation energy of 1.0 ± 0.1 eV is measured, in excellent agreement with the radioactive tracer work.

¹⁹ N. L. Peterson and S. J. Rothman, Phys. Rev. **163**, 645 (1967).

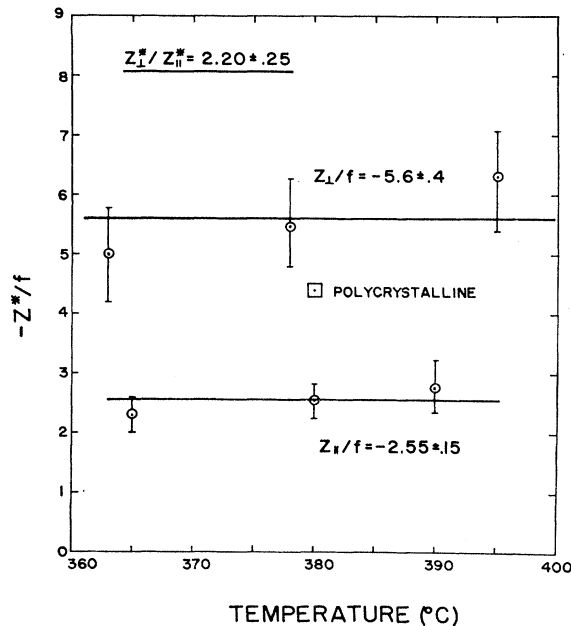


FIG. 10. Z_{\perp}^*/f and Z_{\parallel}^*/f versus temperature ($^{\circ}\text{C}$).

Eq. (7) becomes

$$Z^*/f = -v_m kT / \alpha j \rho D_{sd} |e|, \quad (8)$$

where f is the correlation factor and D_{sd} refers to the self-diffusivity as measured by radioactive tracer experiments.

The results, which we assume are temperature-independent, obtained by using the diffusion data of Peterson and Rothman, are plotted in Fig. 10. The apparent temperature dependence arises because in this experiment the activation energy obtained from the electromigration results is greater than that measured by self-diffusion. Our results are not precise enough to determine whether this effect is real. More precise measurements on other materials (see, for example, Ref. 15) have obtained excellent agreement between the activation energy as measured from electromigration to that measured by self-diffusion. The results are $Z_{\perp}^*/f = -5.6 \pm 0.4$ and $Z_{\parallel}^*/f = -2.55 \pm 0.15$, where the errors are the standard deviations from the mean. Since there is little temperature dependence of the correlation factor in this temperature range and no orientation dependence,²⁰ one calculates $Z_{\perp}^*/Z_{\parallel}^* = 2.20 \pm 0.25$.

The value of $Z^*/f = -4.4 \pm 0.3$ obtained for a polycrystalline specimen is also shown on Fig. 10. As the self-diffusion in Zn is by a vacancy mechanism, one can use $f = 0.78$ and obtain $Z^* = -3.4$, which agrees favorably with the value of -3.0 measured by Thernqvist and Lodding.⁴ It is customary to discuss these results in terms of a total defect resistivity/ $\%$ defect. Combining Eq. (1) and the effective charges quoted above, one obtains $0.3 \mu\Omega \text{ cm}/\%$ defect for \parallel crystals

and $0.5 \mu\Omega \text{ cm}/\%$ defect for the \perp crystals. These values are lower than defect resistivities obtained in simple metals. This is to be expected in a material such as Zn since there are hole and electron charge carriers which transfer momentum in opposite directions.

IV. DISCUSSION

A. Isotropy Factor

One would expect a variation of the dimensional changes and hence also of the α factor with crystallographic orientation. The vacancies which are responsible for the dimensional changes are created or annihilated by the climb of edge dislocations. The radial dimensional changes are greater for \parallel crystals than for \perp ones and hence the isotropy factor is less for \parallel than for \perp crystals. In the case of \parallel crystals, the radial dimensional changes are caused by the climb of basal edge dislocations, while they are edge dislocations lying on prismatic slip systems for \perp specimens. The former dislocations are observed²¹ to climb more easily than the latter and hence cause more radial dimensional changes and a lower α factor.

As mentioned previously, the isotropy factor can only apparently be less than $\frac{1}{3}$ if the surfaces act as vacancy sources or sinks. We have examined the possibility of the oxide film decreasing α . Electron microscopy²² and x-ray topology²³ techniques show that some dislocation loops grow in Zn specimens which have been exposed to air. These observations have been explained by the formation of an oxide, which causes Zn atoms to move to the interface. Accordingly, vacancies are injected into the bulk of the material. This mechanism would cause a uniform increase in the crystal diameter, causing a decreased α on the anode side of the crystal. It cannot explain the $\alpha < \frac{1}{3}$ on the cathode side. Therefore, the vacancy injection mechanism does not adequately describe the results. It is possible that the mechanical constraints imposed by the oxide may be partially responsible for the lower isotropy factor.

Another possible explanation for these lower isotropy factors is that at these temperatures the mean free path of a vacancy is sufficiently long to enable the surfaces to act as sinks. One would need both a very low dislocation density (as might be expected in these high-purity single crystals) and a decreased efficiency of a dislocation to act as a sink at elevated temperatures. Although recent resistivity measurements²⁴ on Au have indicated that above 600°C the sink efficiency of a dislocation is decreased, it seems unlikely that the magnitude of this decrease could lead to a vacancy mean free path of sufficient length to cause the surfaces to become important sinks.

²¹ J. J. Gilman, Trans. Met. Soc. AIME **206**, 1326 (1956).

²² P. S. Dobson and R. E. Smallman, Proc. Roy. Soc. **A293**, 423 (1966).

²³ D. Mitchell and G. J. Ogilvie, Phys. Status Solidi **15**, 83 (1966).

²⁴ C. G. Wang, D. N. Seidman, and R. W. Balluffi, Phys. Rev. **169**, 553 (1968).

²⁰ P. B. Ghate, Phys. Rev. **133**, A1167 (1964).

Solution of the heat equation, considering only generation, conduction, and the area changes due to electromigration, predicts that there should be a shifting of the temperature center with time. This shift is from the geometrical center of the specimen towards the cathode (region of mass depletion). Good agreement was obtained with the shift observed as measured from the velocity center to the original geometrical center. However, it is not possible to determine whether this is an actual temperature shift, as there is only one fixed thermocouple mounted to the crystal. No significant changes in power input or in the slopes of the displacements versus time curves were ever observed. It is possible that the void formation which is probably present may influence the shift.

B. Effective Charges

These measurements are the first to reveal the crystal-line anisotropy of the electromigration driving force. This anisotropy is indeed large. At these temperatures, the diffusivities are anisotropic, $D_{11}/D_{12} \sim 1.6$. Therefore, the anisotropy in the effective charges is in the opposite sense from the diffusivities and overbalances it.

Our results on the effective charge in polycrystalline Zn agree with those reported by Thernqvist and Lodding⁴ and Kuzmenko,⁵ and our single-crystal results bound their values, as was to be expected. Within experimental error this result also obeys $Z_p^* = \frac{1}{3}(2Z_{11}^* + Z_{12}^*)$, where Z_p^* is the effective charge of the polycrystal. This form for the effective charge tensor is also expected. The observed anisotropy and the anode-directed motion would suggest that the anisotropy of the Hall constants would persist at higher temperatures and both would become negative.

Electromigration may be more sensitive to the band structure than conductivity. The conductivity σ is proportional to $\int (\mathbf{A}_k \cdot \mathbf{v}_k / |v_k|) dS_f$, where \mathbf{A} is the mean free path, \mathbf{v} the velocity, and S_f the Fermi surface. Since $\mathbf{A}_k \cdot \mathbf{v}_k$ has the same sign for holes and electrons, the effect of the hole and electron bands are additive. However, in the case of electromigration, the effect of the electrons and holes is competitive, as the effective charge Z^* is proportional to $\int (\mathbf{k} \cdot \mathbf{v}_k / |v_k|) dS_f$, where \mathbf{k} is the electron wave vector and $\mathbf{k} \cdot \mathbf{v}_k$ has opposite signs for electrons and holes. Thus, for a multiband

material the anisotropy in Z^* may be much different from σ .

The results of this study have stimulated a theoretical investigation presently under way. A very tentative model has been used by Feit,²⁵ in which only the 3rd band differs significantly from the free-electron surface. A preliminary calculation shows that the area of the lens is decreased approximately 40% from the free-electron case. Hence the effective charge along the z axis is decreased, and the ratio Z_{11}^*/Z_{12}^* becomes greater than unity, as experimentally observed.

V. SUMMARY

With the marker motion technique, it has been experimentally demonstrated that there is a large anisotropy of electromigration driving force in Zn owing to the band structure. Measurements of the anode-directed drift velocity yield a ratio of the effective charges of $Z_{11}^*/Z_{12}^* = 2.20 \pm 0.25$. The values of Z^* are, respectively, -4.4 for Z_{11}^* and -2.0 for Z_{12}^* . The relative magnitude of these effective charges suggests that there is appreciable compensation between the electron and hole band contributions. It seems that vacancies are created or annihilated preferentially by the climb of edge dislocations lying in basal rather than prismatic planes. The over-all net expansion of the crystal and the isotropy factors less than $\frac{1}{3}$ are not clearly understood.

Comparison of this work with the Hall constant measurements suggests that the constants become more negative at higher temperatures, explaining the direction of mass transport. These results point the need for increased understanding of electromigration based on a more detailed treatment of band structure and transport phenomena.

ACKNOWLEDGMENTS

The author is grateful to Prof. H. B. Huntington, who suggested this problem. His advice and interest during the course of this investigation were of great assistance. The author is also appreciative of many stimulating discussions with J. D'Amico, M. D. Feit, and H. R. Patil.

²⁵ M. D. Feit (private communication).